

Article

Influence of Particulate Reinforcement and Equal-Channel Angular Pressing on Fatigue Crack Growth of an Aluminum Alloy

Lisa Köhler *, Kristin Hockauf and Thomas Lampke

Institute of Materials Science and Engineering, Technische Universität Chemnitz, Erfenschlager Str. 73, 09125 Chemnitz, Germany; E-Mails: kristin.hockauf@mb.tu-chemnitz.de (K.H.); thomas.lampke@mb.tu-chemnitz.de (T.L.)

* Author to whom correspondence should be addressed; E-Mail: lisa.koehler@mb.tu-chemnitz.de; Tel.: +49-371-531-32632; Fax: +49-371-531-23819.

Academic Editor: Heinz Werner Höppel

Received: 26 February 2015 / Accepted: 12 May 2015 / Published: 18 May 2015

Abstract: The fatigue crack growth behavior of unreinforced and particulate reinforced Al 2017 alloy, manufactured by powder metallurgy and additional equal-channel angular pressing (ECAP), is investigated. The reinforcement was done with 5 vol % Al₂O₃ particles with a size fraction of 0.2–2 μm. Our study presents the characterization of these materials by electron microscopy, tensile testing, and fatigue crack growth measurements. Whereas particulate reinforcement leads to a drastic decrease of the grain size, the influence of ECAP processing on the grain size is minor. Both reinforced conditions, with and without additional ECAP processing, exhibit reduced fatigue crack growth thresholds as compared to the matrix material. These results can be ascribed to the well-known effect of the grain size on the crack growth, since crack deflection and closure are directly affected. Despite their small grain size, the thresholds of both reinforced conditions depend strongly on the load ratio: tests at high load ratios reduce the fatigue threshold significantly. It is suggested that the strength of the particle-matrix-interface becomes the critical factor here and that the particle fracture at the interfaces dominates the failure behavior.

Keywords: Al 2017 alloy; Al₂O₃ particulate reinforcement; fatigue crack growth; equal-channel angular pressing (ECAP)

1. Introduction

Aluminum matrix composites (AMCs) are designed to meet the requirements of advanced engineering applications. Reinforcement with ceramic particles provides high strength and stiffness, and enhances wear resistance, thermal stability, and creep resistance [1,2]. It has been shown that methods of severe plastic deformation (SPD) can help to homogenize the particle distribution [3], which improves the mechanical properties. Equal-channel angular pressing (ECAP) has emerged as one of the most frequently used SPD methods for processing particulate reinforced AMCs [4–7]. For unreinforced materials, ECAP processing leads to strain-hardening of the material and decreases the grain size by the rearrangement of dislocations to subgrain boundaries and cell walls [8–10].

Focusing on potential future applications for AMCs produced by ECAP, fatigue crack growth is an important field of interest. To the best of our knowledge, previous studies only focused on crack propagation either in ultrafine-grained materials produced by ECAP or in AMCs. These investigations show the well-known effect of the grain or particle size on the fatigue crack growth. The grain refinement through ECAP leads to a minimized amount of crack deflection and roughness-induced crack closure, which results in higher crack propagation rates and, therefore, in minor thresholds [11–18]. In reinforced materials, particle sizes larger than 2–5 μm have a contrary effect on crack propagation: by increasing crack deflection and roughness-induced crack closure, crack propagation rates are lowered [19–24].

The purpose of the present study is to investigate the influence of particulate reinforcement with a particle size less than 2 μm and additional ECAP on the near-threshold fatigue crack growth of an aluminum alloy. This small particle size was chosen in order to minimize local stress concentrations in the matrix material [25]. It is well-known that small particles cause significantly higher strain hardening and that they are less susceptible to cracking as compared to coarser particles [26,27]. As matrix material, the Al 2017 alloy has been chosen here and in preliminary studies [28], because it combines attractive properties, such as good fracture toughness in the underaged condition, high resistance against crack propagation, and excellent high-temperature strength, which enables future applications for lightweight structures, e.g., for the aerospace and aeronautical industries.

2. Experimental Section

2.1. Material

A commercially available, gas-atomized, spherical Al 2017 powder alloy was used as matrix material. The particle size fraction of the powder, with a chemical composition such as that presented in Table 1, was below 100 μm . Al_2O_3 powder with a particle size fraction of 0.2–2 μm was used as reinforcing component. The composite powder, consisting of 95 vol % matrix material and 5 vol % Al_2O_3 particles, was processed in a high-energy ball mill and hot-degassed at 450 $^\circ\text{C}$ and 0.06 bar for 4 h. Afterwards, compaction was performed by hot isostatic pressing at 450 $^\circ\text{C}$ and 1100 bar for 3 h. The manufacturing process is described in more detail in [28].

Table 1. Chemical composition of the Al 2017 powder alloy.

Element	Al	Cu	Mn	Mg	Fe	Si	Zn
wt %	>94.1	4.1	0.8	0.6	0.2	0.1	traces

The non-ECAP-processed conditions, unreinforced, and reinforced, were solid-solution treated at 505 °C for 60 min, water-quenched, and subsequently naturally aged at room temperature for one month in order to adjust an underaged condition. For the ECAP-processed conditions, as described in [28], a pre-ECAP aging at 140 °C was carried out for 10 min to increase the workability. Immediately after the pre-ECAP aging, the material was ECAP-processed at 140 °C for one pass. The ECAP processing was performed in a device with an internal angle of 120 and a cross-section of $15 \times 15 \text{ mm}^2$, equipped with movable walls and a bottom slider. This processing resulted in an equivalent strain of 0.67 in each passage [29]. After ECAP, the material was peak-aged at 140 °C for 360 min to optimize the ductility. With this combined treatment of ECAP and aging, both elevated strength and moderate ductility can be achieved [30,31].

2.2. Methods of Mechanical Testing and Electron Microscopy

Quasi-static tensile tests were performed in a Zwick-Roell servohydraulic testing machine (Zwick, Ulm, Germany) at a strain rate of $10^{-3} \cdot \text{s}^{-1}$ at room temperature. Cylindrical specimens were used with a cross section of 3.5 mm and a gauge length of 10.5 mm.

Fatigue crack propagation measurements were performed ΔK -controlled in a Rumul testronic resonant testing machine (Russenberger Prüfmaschinen AG, Neuhausen am Rheinfall, Switzerland) at room temperature and at three constant load ratios: $R = 0.1, 0.4$ and 0.7 . Single-edge-notched bend (SEB) specimens with a geometry according to ASTM E399-12e3 [32] and a thickness of 5 mm were used. Figure 1 shows the position in the ECAP billet out of which the SEB specimens were extracted. In the choice of the extraction direction, it was considered that the crack is most likely sidetracked in the direction of the last ECAP shear plane [12]. The crack length was measured continuously according to the principle of the indirect electric potential method with crack measurement foils.

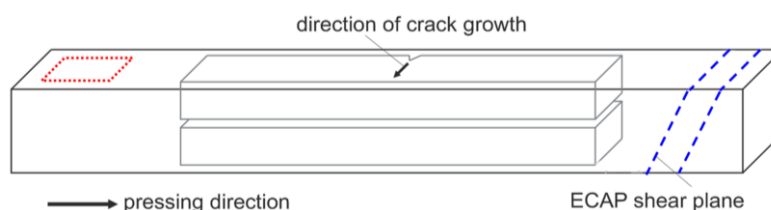


Figure 1. Position of two single-edge-notched bend specimens within the ECAP billet. The ideal direction of crack growth is parallel to the ECAP shear plane. The plane from which samples for microstructural analyses were taken is marked in red.

After precracking at $\Delta K = 2\text{--}7 \text{ MPam}^{1/2}$ (depending on material condition and load ratio), ΔK was lowered in small steps until the fatigue threshold ΔK_{th} was reached. Then, 0.5 mm crack growth were realized at this cyclic stress intensity to avoid any load history effect from the threshold region. In the following, ΔK was raised again in small steps up to a cyclic stress intensity of about $11 \text{ MPam}^{1/2}$ and a crack length of 5 mm.

Samples for microstructural analyses were extracted parallel to the extrusion direction, as shown in Figure 1, and electro-polished followed by a final ion milling polishing step. These samples were analyzed by scanning transmission electron microscopy (STEM) and quadrant back scatter diffraction (QBSD) at an accelerating voltage of 30 kV, as well as by electron back scatter diffraction (EBSD, EDAX TSL

OIM 5.2, AMETEK GmbH, Wiesbaden, Germany) at 15 kV using a Zeiss Neon 40 field emission microscope (Carl Zeiss MicroImaging GmbH, Jena, Germany).

3. Results and Discussion

3.1. Tensile Tests

The tensile properties of the investigated material conditions are shown in Table 2. The unreinforced aluminum matrix (in an underaged heat treatment condition) exhibits the lowest yield strength with 252 MPa just as the highest ductility, which shows in a uniform elongation of 20%. ECAP processing (with subsequent aging as described in the experimental section) leads to a significant increase in yield strength (487 MPa, which is an increase of 93%) in combination with a moderate ductility (11% uniform elongation). The strategy of combining ECAP and aging, which is used here and which is referred to as “optimizing heat treatment” in [33], enables this favorable combination of strength and ductility: ECAP processing results in a severely strain hardened material with a high dislocation density. In the following process of thermal aging, numerous finely-dispersed precipitates form and strengthen the matrix. Simultaneously, thermal recovery takes place and increases the material’s ductility.

Table 2. Tensile properties of the unreinforced and reinforced conditions.

Material	Yield Strength in MPa	Ultimate Tensile Strength in MPa	Uniform Elongation in %	Elongation to Fracture in %
Al 2017 unreinforced	252	435	20	29
Al 2017 unreinforced after 1 ECAP pass	487	566	11	17
Al 2017 with 5 vol % Al ₂ O ₃	328	511	11	13
Al 2017 with 5 vol % Al ₂ O ₃ after 1 ECAP pass	509	580	5	8

The dispersion strengthening, which is caused by the reinforcement with 5 vol % particles, leads to an improvement in strength, which is less compared to the strengthening, which is achieved by ECAP of the unreinforced material. ECAP processing of the particulate reinforced material increases the yield strength from 328 MPa to 509 MPa (which is an increase of 55%). This shows, that the effect of strain hardening during ECAP is less pronounced than in the unreinforced material. Both reinforced conditions exhibit minor ductility, which is ascribed to the particles which act as interior notches [28].

3.2. Microstructure

One ECAP pass of the unreinforced matrix material leads to a bimodal grain structure with inhomogeneously distributed refined grains. The initial grain size is significantly reduced in the shear bands, which is shown in Figure 2. In the outside parts, almost no grain refinement has taken place.

The reinforced material exhibits elongated areas with a width of 100–200 μm and a height of about 7 μm without reinforcement components. These areas are preferentially orientated parallel to the direction of extrusion. In Figure 3, micrographs of the reinforced areas are shown. The Al₂O₃ particles are finely dispersed and exhibit an intact interface to the aluminum matrix. In these micrographs, the presence of the coarse intermetallic phase Al₂Cu can also be seen. Additional ECAP does not lead to significant grain refinement (see Figure 4).

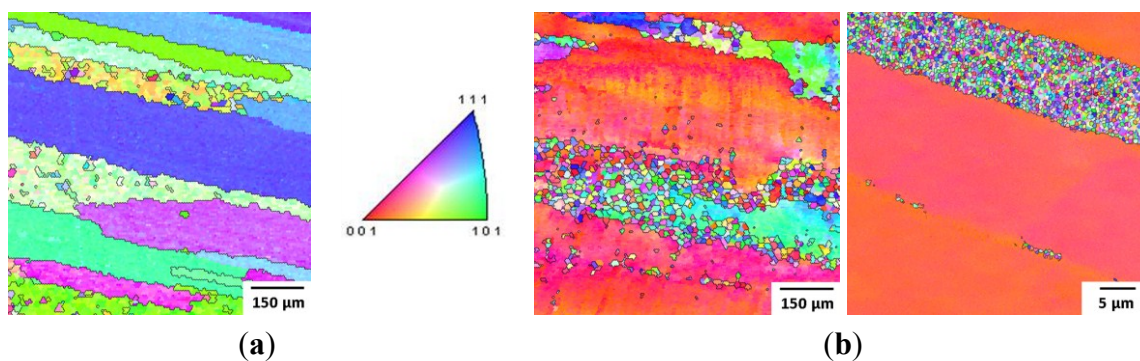


Figure 2. Electron back scatter diffraction (EBSD) color-coded orientation maps of the unreinforced matrix material conditions: **(a)** non-ECAP-processed and **(b)** after one ECAP pass. In the shear bands, the grain size is considerably reduced after one ECAP pass. By contrast, the initial grain size outside the shear bands is almost maintained.

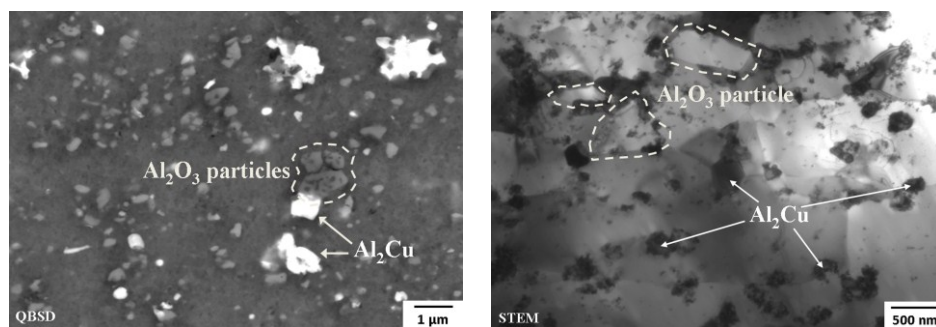


Figure 3. Quadrant backscatter diffraction (QBSD, **left**) and scanning transmission electron microscopy (STEM, **right**) micrographs of Al 2017 with 5 vol % Al_2O_3 particles with a size of 0.2–2 μm . Al_2O_3 particles are marked with broken lines and the Al_2Cu precipitates with arrows. The particles are finely dispersed and matrix and particles exhibit an intact interface.

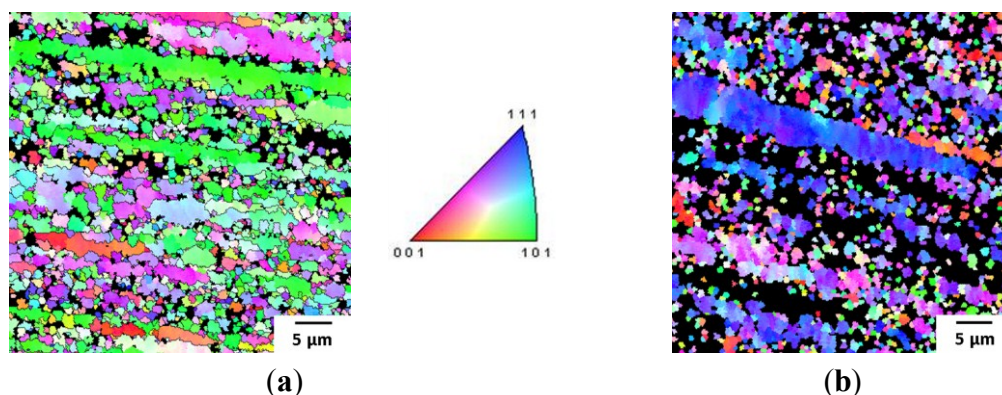


Figure 4. EBSD color-coded orientation maps of the reinforced conditions: **(a)** non-ECAP-processed and **(b)** after additional ECAP. For the reinforced material, ECAP does not lead to a significant grain refinement.

3.3. Fatigue Crack Surface Analysis

For the unreinforced conditions the fatigue crack surfaces are shown in Figure 5. The non-ECAP-processed condition exhibits a strongly faceted surface with pronounced band-typed steps. This fissured crack surface can be explained by the large grain size of this condition and thus by a high amount of crack deflection. For the material after one ECAP pass, plateaus are present on the crack surface. Additionally, striations are clearly visible. Such signs of “micro-damage” have also been observed for other ECAP-processed aluminum alloys [16]. They were interpreted as the severely strain-hardened material is not being able to compensate the stresses at the crack tip by deforming plastically. Compared to the unprocessed material, the crack path after ECAP is less tortuous and more straight-forward. Presumably, the crack propagates preferably along or within the shear bands.

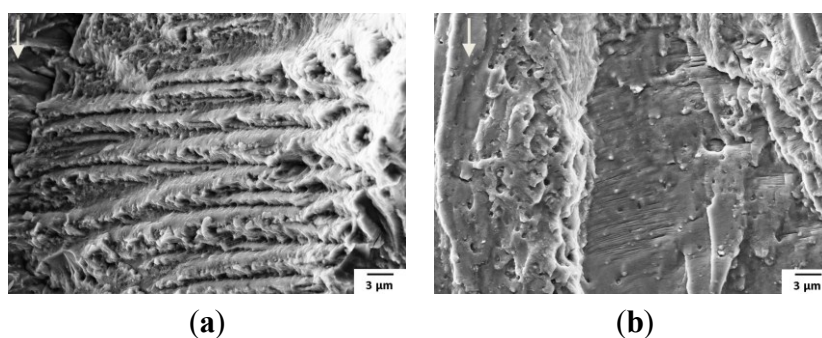


Figure 5. Fatigue crack surfaces of the unreinforced conditions: (a) non-ECAP-processed and (b) after one ECAP pass near the fatigue threshold. The crack propagation direction is marked with an arrow. The surface of the non-ECAP-processed condition exhibits a band-type faceted appearance, whereas ECAP leads to plateaus and clearly visible striations.

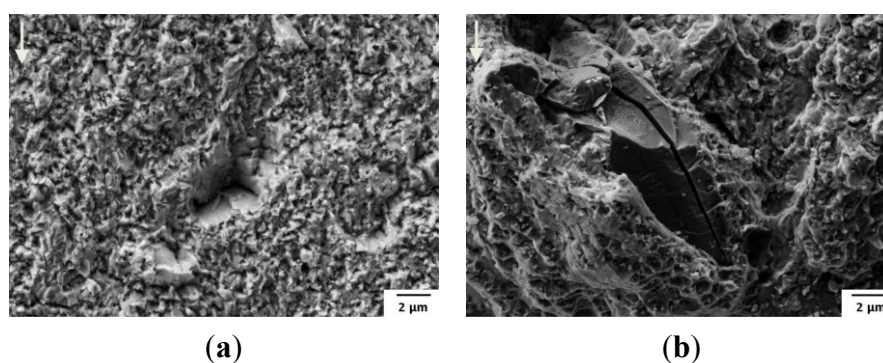


Figure 6. Fatigue crack surfaces of the reinforced conditions: (a) non-ECAP-processed and (b) after one ECAP pass near the fatigue threshold. The crack propagation direction is marked with an arrow. The surface is less rough and barely fissured as compared to the unreinforced conditions. Through additional ECAP, the particle failure is more likely to fracture than to break out.

In Figure 6, the fatigue crack surfaces of the reinforced conditions are shown. In contrast to the unreinforced conditions, the crack surfaces are characterized by a minor roughness. Hardly any faceting is noticeable. Due to the small grain and particle sizes of these conditions, crack deflection is reduced to

a minimum. This outcome is in good agreement with the findings in [19,34]. It is noticeable that, in the ECAP-processed condition, particle fracture is more pronounced, whereas the initial reinforced condition exhibits a higher rate of particle break outs. It cannot be concluded with certainty if the particle fracture proceeded due to fatigue loading or whether it was caused by ECAP.

3.4. Fatigue Crack Propagation

Fatigue crack growth curves near the threshold for the tested load ratios are shown in Figure 7. The matrix material exhibits the highest thresholds and the lowest fatigue crack growth rates for all tested conditions. Due to the major grain size of the matrix material, the amount of crack deflection and roughness-induced crack closure and, therefore, the strongly branched crack path lead to decreased fatigue crack growth rates, which results in major thresholds. One ECAP pass results in higher crack growth rates and lower thresholds. Presumably, due to the preferred crack propagation along the shear bands and the finer grains in this area, less crack deflection and closure occurs. Supposedly, also the high dislocation density induced by ECAP inhibits stress relief and, therefore, early damaging at the crack tip takes place [13].

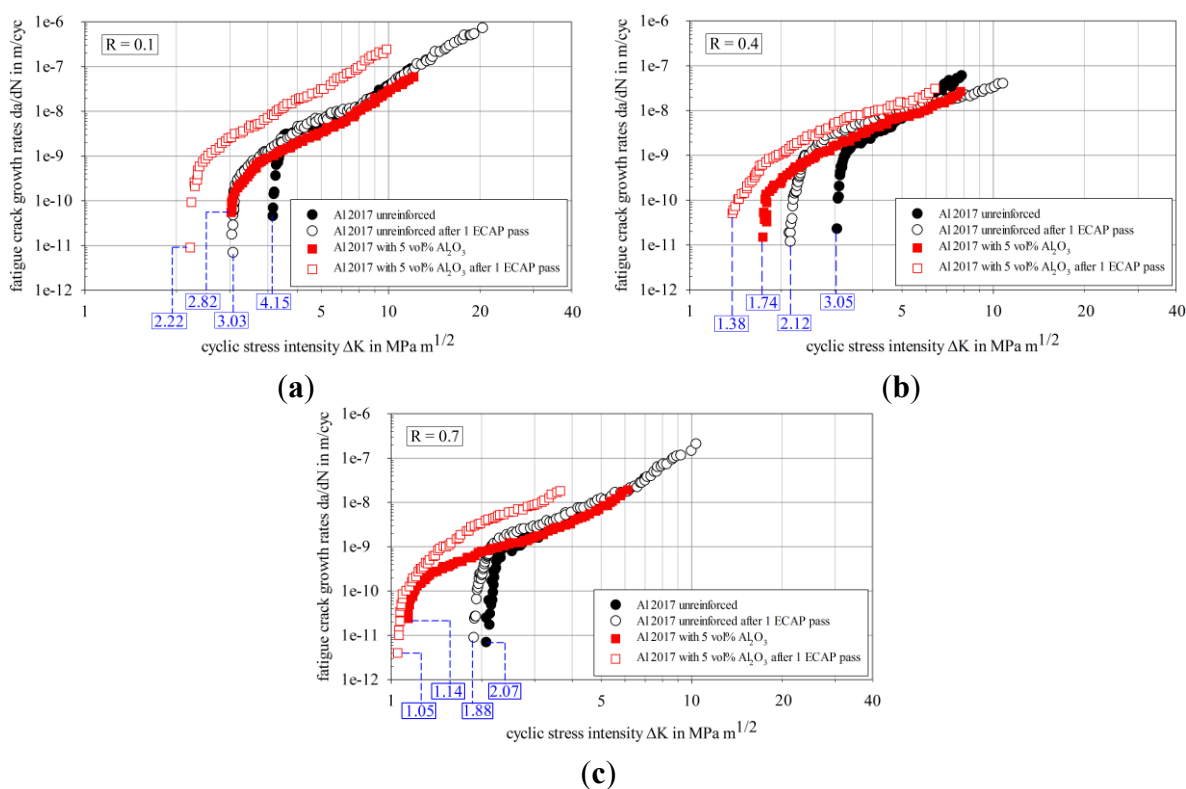


Figure 7. Fatigue crack growth curves of Al 2017 in unreinforced and reinforced conditions with additional ECAP at load ratios of: (a) $R = 0.1$, (b) $R = 0.4$, and (c) $R = 0.7$. The thresholds for the reinforced conditions are lower than for the matrix material conditions. With the increase of the load ratio, this effect becomes more pronounced. The crack growth rates for the reinforced ECAP-processed conditions are generally the highest.

For the reinforced conditions, at low cyclic stress intensities, the crack propagation rates are higher as compared to the matrix material conditions. As the near threshold regime is highly sensitive to the

microstructure, the main factor for this behavior is presumably the significantly smaller grain size and the resulting minimized effects of crack deflection and roughness-induced crack closure. For the ECAP-processed conditions, fatigue crack growth thresholds are further reduced as compared to their corresponding not-processed conditions. This is probably due to the high dislocation density in these materials, which leads to a diminished deformation ability at the crack tip.

Figure 8 presents the fatigue threshold depending on the load ratio for all tested conditions. The matrix material and both reinforced conditions exhibit a strong dependency on the load ratio. Although the curve progression is nearly parallel for these three conditions, the underlying mechanisms are different. The matrix material shows the highest thresholds and also a strong load ratio dependency. This can be explained by the well-known effect of the grain size on the crack growth at different load ratios [11–13,15,35]. The amount of crack deflection is constant for all load ratios, whereas the effect of roughness induced crack closure is minimized by increasing the load ratio. The fatigue thresholds of the ECAP-processed matrix material show a minor dependency on the load ratio. Supposedly, the small grain size in the shear bands and therefore the generally low amount of crack deflection and closure lead here to minimized load ratio effects.

However, despite their small grain size, both reinforced conditions exhibit a strong dependency on the load ratio. In this case, assumedly, the thresholds depend critically on the interaction between the softer aluminum matrix where crack propagation takes place and the interface where decohesion or brittle particle fracture can occur [36]. At higher load ratios, the susceptibility to cracking of the particle-matrix-interface is strongly increased. On that account, fatigue thresholds further decrease for higher load ratios. This, in turn, results in a higher load-ratio-dependency. For the reinforced condition, additional ECAP does not influence the load ratio dependency.

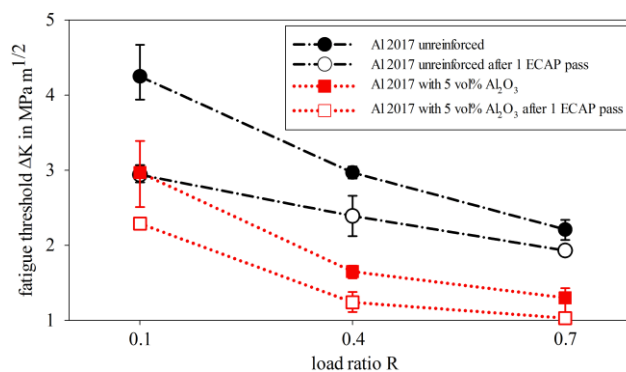


Figure 8. Fatigue thresholds of Al 2017 in unreinforced and reinforced conditions with additional ECAP at different load ratios. The ECAP-processed matrix material exhibits the least dependency on the load ratio. In contrast, the matrix material and the reinforced conditions depend strongly on the load ratio and display almost the same amount for the three conditions.

4. Conclusions

In this paper, the effect of particulate reinforcement and equal-channel angular pressing on the fatigue crack growth in an aluminum alloy produced by powder metallurgy is investigated. For the Al 2017 powder alloy, reinforced with 5 vol % Al₂O₃ with a size fraction of 0.2–2 μm, the fatigue properties are

compared to the unreinforced material. Two different conditions for both materials are chosen: non-processed and after one pass of ECAP.

- (1) One ECAP pass of the unreinforced material results in an inhomogeneous microstructure with shear bands. These shear bands are characterized by a considerably reduced grain size. In the surrounding areas, the grains are strongly elongated, but not refined. The grain size of the reinforced material is significantly lower, as compared to the unreinforced. Additional ECAP does not lead to a significant grain refinement, here.
- (2) The yield strength of both materials, unreinforced and reinforced, is increased by one pass of ECAP. However, the strain hardening effect of ECAP is more pronounced in the unreinforced material.
- (3) Due to the major grain size of the unreinforced matrix material, the high amount of crack deflection and roughness-induced crack closure lead to a tortuous crack path and therefore to minor crack propagation rates. The grain refinement through one ECAP pass reduces these effects. Supposedly because crack propagation occurred in the finer-grained shear bands, the fatigue thresholds and their dependency on the load ratio are diminished for the unreinforced material after ECAP.
- (4) For the reinforced material, the fatigue thresholds are drastically reduced due to the significantly smaller grain size of these conditions. Despite their small grain size, the reinforced materials exhibit a strong dependency on the load ratio. Here, the interaction between the aluminum matrix and the interface is perceived as crucial: the susceptibility to cracking of the particle-matrix-interface is strongly increased at higher load ratios. This leads to a “particle-failure-induced” load ratio dependency.

Acknowledgments

The authors gratefully acknowledge funding of the Collaborative Research Center SFB 692 received from the German Research Foundation (Deutsche Forschungsgemeinschaft DFG).

Author Contributions

L.K. performed and analyzed the experiments and is the primary author of the paper. K.H. conceived and designed the experiments and discussed the results and analysis with the author. T.L. supervised the work.

Conflicts of Interest

The authors declare no conflict of interest.

References

1. Chawla, N.; Shen, Y.L. Mechanical behavior of particle reinforced metal matrix composites. *Adv. Eng. Mater.* **2001**, *3*, 357–370.
2. Mani, B.; Paydar, M.H. Application of forward extrusion-equal channel angular pressing (FE-ECAP) in fabrication of aluminum metal matrix composites. *J. Alloys Compd.* **2010**, *492*, 116–121.

3. Tan, M.J.; Zhang, X. Powder metal matrix composites: Selection and Processing. *Mater. Sci. Eng. A* **1998**, *244*, 80–85.
4. Ramu, G.; Bauri, R. Effect of equal channel angular pressing (ECAP) on microstructure and properties of Al-SiC_p composites. *Mater. Des.* **2009**, *30*, 3554–3559.
5. Sabirov, I.; Kolednik, O.; Valiev, R.Z.; Pippan, R. Equal channel angular pressing of metal matrix composites: Effect on particle distribution and fracture toughness. *Acta Mater.* **2005**, *53*, 4919–4930.
6. Valiev, R.Z.; Islamgaliev, R.K.; Kuzmina, N.F.; Li, Y.; Langdon, T.G. Strengthening and grain refinement in an Al-6061 metal matrix composite through intense plastic straining. *Scr. Mater.* **1999**, *40*, 117–122.
7. Muñoz-Morris, M.A.; Calderón, N.; Guitierrez-Urrutia, I.; Morris, D.G. Matrix grain refinement in Al-TiAl composites by severe plastic deformation: Influence of particle size and processing route. *Mater. Sci. Eng. A* **2006**, *425*, 131–137.
8. Segal, V.M.; Reznikov, V.I.; Drobyshevskiy, A.E.; Kopylov, V.I. Plastic working of metals by simple shear (Russian translation). *Russ. Metall.* **1981**, *1*, 99–105.
9. Valiev, R.Z.; Langdon, T.G. Principles of equal-channel pressing as a processing tool for grain refinement. *Prog. Mater. Sci.* **2006**, *51*, 881–981.
10. Furukawa, M.; Horita, Z.; Langdon, T.G. Developing ultrafine grain sizes using severe plastic deformation. *Adv. Eng. Mater.* **2001**, *3*, 121–125.
11. Pao, P.S.; Jones, H.N.; Cheng, S.F.; Feng, C.R. Fatigue crack propagation in ultrafine grained Al-Mg alloy. *Int. J. Fatigue* **2005**, *27*, 1164–1169.
12. Hübner, P.; Kiessling, R.; Biermann, H.; Hinkel, T.; Jungnickel, W.; Kawalla, R.; Höppel, H.-W.; May, J. Static and cyclic crack growth behavior of ultrafine-grained Al produced by different severe plastic deformation methods. *Metall. Mater. Trans. A* **2007**, *38*, 1926–1933.
13. Vinogradov, A. Fatigue limit and crack growth in ultra-fine grain metals produced by severe plastic deformation. *J. Mater. Sci.* **2007**, *42*, 1797–1808.
14. Cavaliere, P. Fatigue properties and crack behavior of ultra-fine and nanocrystalline pure metals. *Int. J. Fatigue* **2009**, *31*, 1476–1489.
15. Estrin, Y.; Vinogradov, A. Fatigue behaviour of light alloys with ultrafine grain structure produced by severe plastic deformation: An overview. *Int. J. Fatigue* **2010**, *32*, 898–907.
16. Meyer, L.W.; Sommer, K.; Halle, T.; Hockauf, M. Crack growth in ultrafine-grained AA6063 produced by equal-channel angular pressing. *J. Mater. Sci.* **2008**, *43*, 7426–7431.
17. Avtokratova, E.V.; Sitdikov, O.S.; Kaibyshev, R.O.; Watanabe, Y. Behavior of a submicrocrystalline aluminum alloy 1570 under conditions of cyclic loading. *Phys. Met. Metallogr.* **2009**, *107*, 291–297.
18. Hockauf, K.; Wagner, M.F.-X.; Halle, T.; Niendorf, T.; Hockauf, M.; Lampke, T. Influence of precipitates on low-cycle fatigue and crack growth behavior in an ultrafine-grained aluminum alloy. *Acta Mater.* **2014**, *80*, 250–263.
19. Chen, Z.Z.; Tokaji, K. Effects of particle size on fatigue crack initiation and small crack growth in SiC particulate-reinforced aluminum alloy composites. *Mater. Lett.* **2004**, *58*, 2314–2321.
20. Levin, M.; Karlsson, B. Influence of SiC particle distribution and prestraining on fatigue crack growth rates in aluminum AA 6061-SiC composite material. *Mater. Sci. Technol.* **1991**, *7*, 596–607.

21. Mason, J.J.; Ritchie, R.O. Fatigue crack growth resistance in SiC particulate and whisker reinforced P/M 2124 aluminum matrix composites. *Mater. Sci. Eng. A* **1997**, *231*, 170–182.
22. Llorca, J. Fatigue of particle- and whisker-reinforced metal-matrix composites. *Prog. Mater. Sci.* **2002**, *47*, 283–353.
23. Oh, K.H.; Han, K.S. Short-fiber/ particle hybrid reinforcement: Effects on fracture toughness and fatigue crack growth of metal matrix composites. *Comput.. Sci. Technol.* **2007**, *67*, 1719–1726.
24. Chawla, N.; Ganesh, V.V. Fatigue crack growth of SiC particle reinforced metal matrix composites. *Int. J. Fatigue* **2010**, *32*, 856–863.
25. Huang, M.; Li, Z. Size effects on stress concentration induced by a prolate ellipsoidal particle and void nucleation mechanism. *Int. J. Plast.* **2005**, *21*, 1568–1590.
26. Xue, Z.; Huang, Y.; Li, M. Particle size effect in metallic materials: A study by the theory of mechanism-based strain gradient plasticity. *Acta Mater.* **2002**, *50*, 149–160.
27. Slipenyuk, A.; Kuprin, V.; Milman, Y.; Goncharuk, V.; Eckert, J. Properties of P/M processed particle reinforced metal matrix composites specified by the reinforcement concentration and matrix-to-reinforcement particle size ratio. *Acta Mater.* **2006**, *54*, 157–166.
28. Wagner, S.; Siebeck, S.; Hockauf, M.; Nestler, D.; Podlesak, H.; Wielage, B.; Wagner, M.F.X. Effect of SiC-reinforcement and equal-channel angular pressing on microstructure and mechanical properties of AA2017. *Adv. Eng. Mater.* **2012**, *14*, 388–393.
29. Iwahashi, Y.; Wang, J.T.; Horita, Z.; Nemoto, M.; Langdon, T.G. Principle of equal-channel angular pressing for the processing of ultra-fine grained materials. *Scr. Mater.* **1996**, *35*, 143–146.
30. Kim, J.K.; Jeong, H.G.; Hong, S.I.; Kim, Y.S.; Kim, W.J. Effect of aging treatment on heavily deformed microstructure of a 6061 aluminum alloy after equal channel angular pressing. *Scr. Mater.* **2014**, *45*, 901–907.
31. Hockauf, M.; Meyer, L.W.; Zillmann, B.; Hietschold, M.; Schulze, S.; Krüger, L. Simultaneous improvement of strength and ductility of Al-Mg-Si alloys by combining equal-channel angular extrusion with subsequent high-temperature short-time aging. *Mater. Sci. Eng. A* **2009**, *503*, 167–171.
32. ASTM E399-12e3. *Standard Test Method for Linear-elastic Plane-Strain Fracture Toughness K_{Ic} of Metallic Materials*. American Society for Testing and Materials: West Conshohocken, PA, USA, 1970.
33. Hockauf, M.; Schönherr, R.; Wagner, S.; Meyer, L.W.; Podlesak, H.; Mücklich, S.; Wielage, B.; Krüger, L.; Hahn, F.; Weber, D. Equal-channel angular pressing of medium- to high-strength precipitation hardening aluminium wrought alloys. *Mat.-Wiss. Werkstofftech.* **2009**, *40*, 540–550.
34. Shang, J.K.; Ritchie, R.O. On the particle-size dependence of fatigue-crack propagation thresholds in SiC-particulate-reinforced aluminium alloy composites: Role of crack closure and crack trapping. *Acta Metall.* **1989**, *37*, 2267–2278.
35. Hockauf, K.; Halle, T.; Hockauf, M.; Wagner, M.F.-X.; Lampke, T. Near-threshold fatigue crack propagation in an ECAP-processed ultrafine-grained aluminium alloy. *Mater. Sci. Forum* **2011**, *667–669*, 873–878.

36. Shang, J.K.; Yu, W.; Ritchie, R.O. Role of silicon carbide particles in fatigue crack growth in SiC-particulate-reinforced aluminum alloy composites. *Mater. Sci. Eng. A* **1988**, *102*, 181–192.

© 2015 by the authors; licensee MDPI, Basel, Switzerland. This article is an open access article distributed under the terms and conditions of the Creative Commons Attribution license (<http://creativecommons.org/licenses/by/4.0/>).